GU J Sci, Part C, 10(3): 455-467 (2022)

Gazi University

Journal of Science

PART C: DESIGN AND TECHNOLOGY

http://dergipark.gov.tr/gujsc

Improving the Mechanical Properties of GPLs-SiAlON Composites by Microfluidization Technique as a New Approach to Dispersion of GPLs

Sinem BAŞKUT[1*] Servet TURAN[1,2]

[1]*Eskisehir Technical University, Faculty of Engineering, Department of Materials Science and Engineering, 26555, ESKİSEHİR*

[2]*MDA Advanced Ceramics, Organize Sanayi Bolgesi Teknoloji Bulvarı, 26250, ESKİSEHİR*

Article Info

Research article
Received: 12.05.2022
Revision: 13.06.2022
Accepted: 29.06.2022

Keywords

Graphene platelets (GPLs)
Microfluidization
Thickness of GPLs
Fracture toughness

Abstract

Graphene platelets (GPLs) are frequently preferred as reinforcement material to improve the mechanical properties of many advanced technology ceramics, thanks to their superior properties. However, their reinforcement levels vary depending on whether they are homogeneously distributed in the matrix microstructure. This is generally controlled by the thickness (number of layers) of the GPLs. In general, single- or few-layer GPLs show high performance as reinforcement but are commercially expensive. This limits their large-scale use. This study aims to achieve the performance of the GPLs (GPL_{Ref}), which is determined to have a high mechanical reinforcement level but is quite expensive, by economically thinning other GPLs (C0-GPL) with similar platelet size but thicker structure and cheaper. For this purpose, the microfluidization technique, a new approach to the dispersion of GPLs, was applied. C0-GPL was exposed to 1, 2, 4 and 8 cycles of microfluidization process. Microfluidized GPLs were added to the SiAlON matrix at a ratio of 1.5 wt %, and the GPLs-SiAlON composites were sintered using the spark plasma sintering (SPS) technique. The platelet size of C0-GPL decreased as the number of applied microfluidization cycles increased. However, while this reduction in platelet size was not significant up to 2 cycles, it was very pronounced at 4 and 8 cycles. Raman analyses revealed that GPLs could be dispersed effectively for up to 4 cycles. After this point, the GPLs fragmented rather than thin as the number of cycles increased. GPLs, slightly thinner than GPL_{Ref} could be obtained with 2 cycles of microfluidization (C2-GPL). Therefore, C2-GPL were more homogeneously dispersed in SiAlON matrix microstructure compared to GPL_{Ref}. As a result, both the through-plane and in-plane direction fracture toughness values of SiAlON matrix containing C2-GPL, which partially preserved the platelet size, were higher than those of GPL_{Ref}-SiAlON. The fracture toughness of SiAlON matrix composites containing 4 and 8 cycles of microfluidized GPLs were lower than that of GPL_{Ref}-SiAlON as an adverse effect of decreasing platelet size. It has been determined that the mechanical reinforcement performance of commercially expensive GPL_{Ref} can be achieved economically by applying 2 cycles of microfluidization to cost-effective C0-GPL.

1. INTRODUCTION

GPLs are frequently used as reinforcement material in recent years due to their high surface area and superior mechanical properties (high fracture strength (~125 GPa) and Young's modulus (~1TPa)) [1-3]. It has been determined that the mechanical properties of many advanced technology ceramics, such as fracture toughness and flexural strength, are improved with the addition of GPLs. Study [4] in which 0.2, 0.5, 1, 2, 5 and 10 wt % GPLs were added to Si_3N_4, the fracture toughness and strength of the matrix increased by approximately 9 and 3 %, respectively, at 0.2 wt % GPLs content. In another study [5], the fracture toughness of zirconia increased by about 30 % with the addition of 4 vol % graphene oxide. The fracture toughness and flexural strength of Al_2O_3 matrix improved by 27 and 30 %, respectively, at 0.38 vol % GPLs content in a study conducted on GPLs-Al_2O_3 composites [6]. SiAlON, an alloy of silicon nitride (Si_3N_4), is included in the advanced technology ceramics group. It has industrial applications such as metal forming tools, milling media, blast nozzles, cutting tools, thermocouple protection tubes, riser, and heater tubes [7-9]. On the other hand, when its mechanical properties improve, its usage areas will increase and diversify.

*Corresponding author, e-mail: skayhan@eskisehir.edu.tr
DOI:10.29109/gujsc.1115494

For this purpose, the addition of GPLs to SiAlON as a reinforcement material is one of the appropriate strategies.

This study is a continuation of the study [10] investigating the effects of adding four GPLs with different properties such as size, thickness, and aspect ratio on the mechanical and tribological properties of the SiAlON matrix. In that study, the largest and thinnest GPLs (called GPL4) among the added GPLs provided the highest fracture toughness and tribological properties to SiAlON. However, the fact that the commercial price of these GPLs (GPL4) with good exfoliation is quite high compared to the others has limited its high-scale use. In that study, GPLs (called GPL3) with almost the same platelet size as GPL4 but thicker and cheaper exhibited a second higher mechanical reinforcement effect following the GPL4. The reason for the higher mechanical and tribological contribution of GPL4 to SiAlON compared to GPL3 was their more homogeneously dispersion in the matrix microstructure caused by their thinner structure. Therefore, the motivation of this study was to investigate whether the reinforcement level of GPL4 could be reached in economical ways by making GPL3 thinner/few-layered. The literature survey revealed that sonication, ball milling and centrifuge techniques are generally applied alone or in combination for the dispersing or thinning the GPL agglomerates [11-14]. However, the implementation of these techniques requires time.

In this study, the microfluidization technique, a new approach for the dispersing or thinning GPLs, was applied as an alternative to traditional techniques. Microfluidization is a technique that provides homogenization of particles under the influence of cavitation, shear and impact forces [15]. In the microfluidization process, the product loaded into the inlet reservoir is pumped into the interaction chamber, including fixed or different geometry microchannels, with the help of constant high pressure [16]. Particles exposed to processing in microchannels under the influence of various forces are collected in the outlet reservoir. The exfoliation process with microfluidization takes place faster than the sonication, ball milling and centrifuge techniques [17]. For the purpose of this study, commercially cheap GPL3 used in the previous study [10] were exposed to 1, 2, 4 and 8 cycles of microfluidization processes. All GPLs were added to the SiAlON matrix in the same amount and GPLs-SiAlON composites were produced using the SPS technique. Scanning electron microscopy (SEM), Raman analyses and the density, hardness, and fracture toughness measurements were performed.

2. MATERIALS AND METHODS

2.1. PRODUCTION OF THE MATERIALS

The GPLs (called GPL4 in the previous study) whose few-layered structure is desired to be reached in the study are called as GPL_{Ref} (Graph. Chem. Ind. Comp.), and the cheap GPLs (called GPL3 in the previous study) to be microfluidized are named as C0-GPL (Graph. Chem. Ind. Comp.) during the study. Table 1 shows the properties of these two GPLs. C0-GPL was firstly dispersed for 1 h using the probe-sonication technique (Sonics, 750 Vef). Then, they were exposed to 1, 2, 4 and 8 cycles of microfluidization (Microfluidics Corp.) under constant pressure (1590 bar). GPLs prepared in 1, 2, 4 and 8 cycles are named as C1-GPL, C2-GPL, C4-GPL and C8-GPL, respectively. Platelet sizes and surface areas of the C0-GPL and microfluidized GPLs were measured. Isopropanol was removed from the microfluidized GPLs using a rotary evaporator (Heidolph).

Table 1. *The properties of the GPL_{Ref} and C0-GPL [18, 19, 25].*

GPLs	Average Size (μm)	Thickness (nm)	Aspect Ratios	Purity (%)
GPL_{Ref}	12.62 (5.40-30.45)	0.8-1.2	6,550-25,000	99.8
C0-GPL	12.22 (5.40-30.15)	5-8	675-3,770	99.9

The α-Si_3N_4 (UBE Industries Ltd., Japan), AlN (Tokuyama, H type, d50: 2-2.4 μm, Japan), Al_2O_3 (Alcoa-A16SG), Y_2O_3 (99,9 % purity, H.C. Starck Berlin, Germany), $CaCO_3$ (Reidel-de Haen, Germany), Sm_2O_3

(99.9 % purity, Stanford Materials Corp., USA), were the powders forming the SiAlON matrix. SiAlON matrix composition was composed of 91 % Si_3N_4 powder and 9 % sintering additives. GPL_{Ref}, C0-GPL and microfluidized GPLs were added to SiAlON matrix powder at a ratio of 1.5 wt %. Powder mixtures were blended with 3 h probe-sonication in an isopropanol medium followed by planetary ball milling (Fritsch, Pulverisette) for 1.5 h at 300 rpm. The isopropanol removed from the slurries in a rotary evaporator. The SiAlON matrix and GPLs-SiAlON's powders were sintered using SPS (HP 25D, FCT GmbH) at 1800 °C with a uniaxial pressure of 50 MPa for 15 min under a vacuum atmosphere following the sieving process [18]. The produced samples had a diameter of 20 mm and a thickness of 6 mm.

2.2. CHARACTERIZATION OF THE MATERIALS

Due to the uniaxial pressure applied in the SPS causing the most of GPLs to be oriented in the matrix microstructure, samples were cut in the direction parallel and perpendicular to the SPS pressing axis. Measurements were carried out in the directions through-plane (//, parallel to the SPS pressing axis) and in-plane (⊥, perpendicular to the SPS pressing axis). Figure 1 explains measurement directions.

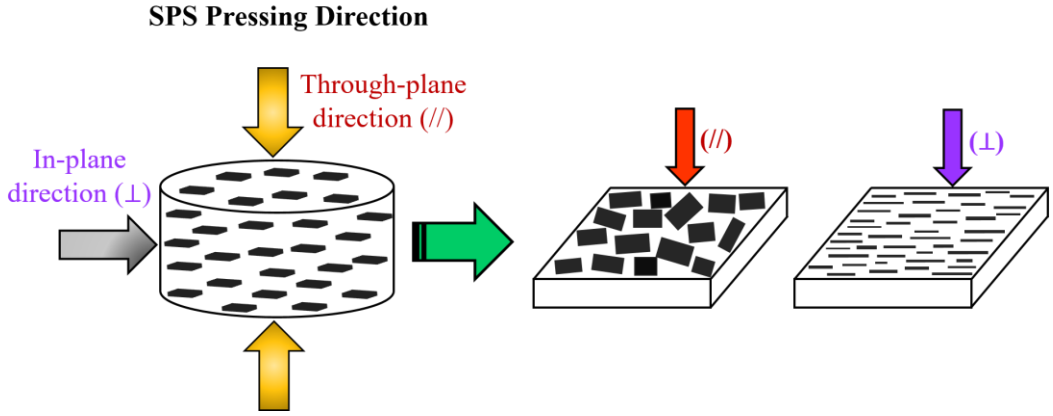

Figure 1. *Measurement directions depending on the SPS pressing axis.*

The samples were molded with Bakelite and mechanically polished for investigations. The morphological secondary electron (SE-SEM) images of GPL_{Ref}, C0-GPL and microfluidized GPLs, in-plane direction backscatter electron (BSE-SEM) images of the produced samples were obtained in the SEM (Zeiss, SUPRA 50 VP). In addition, the Raman (WITec, alpha 300) analyses were performed on GPL_{Ref}, C0-, C1-, C2, C4- and C8-GPLs.

The bulk density values were measured by using the Archimedes method. Additionally, relative density values were calculated based on the volume-based rule of mixtures. For this, the bulk density of SiAlON and GPLs used as 3.23 and 2.26 gcm^{-3}, respectively.

At least ten hardness measurements (Emco-Test) were made on the mechanically polished samples in the through-plane and in-plane directions under the conditions of 3 kg load for 10 s dwell time, and their average values were used in the study. The fracture toughness values were calculated using the Niihara equation [20].

3. RESULTS AND DISCUSSION

3.1. MICROSTRUCTURE AND DENSITY INVESTIGATIONS

Figure 2 presents morphological SE-SEM images of GPL_{Ref}, non-microfluidized C0-GPL and 1, 2, 4 and 8 cycles of microfluidized GPLs. Platelet size measurements given elsewhere [19] and morphological images were compatible with each other. It was determined that the platelet sizes of GPL_{Ref} (Fig. 2 a) and C0-GPL (Fig. 2 b) were close to each other, and the platelet size of C0-GPL decreased in the range of ~13-65 % as the number of microfluidization cycles increased [19]. This revealed that cavitation, shear and impact forces in the interaction chamber led to the fragmentation of the GPLs. On the other hand, the surface area values of the C0-GPL increased as the applied microfluidization cycles increased (Table 2). Surface area values

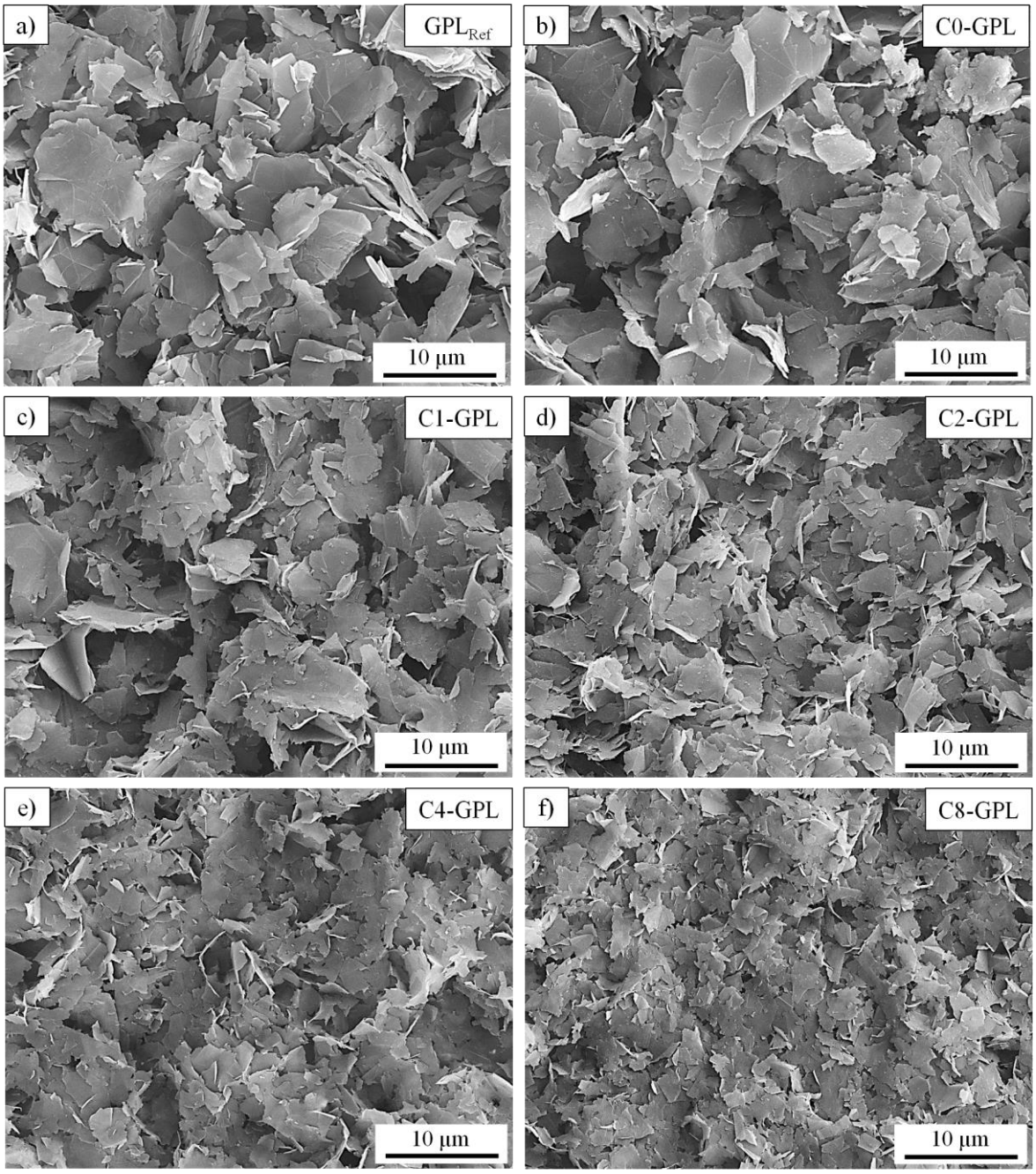

Figure 2. *Morphological SE-SEM images of the (a) GPL_{Ref}, (b) non-microfluidized CO-GPL and (c) 1, (d) 2, (e) 4 and (f) 8 cycle of microfluidized GPLs [18].*

T*able 2.* *The surface area values of the GPL_{Ref} ,C0-GPL and microfluidized GPLs [18].*

GPLs	Surface Area (m^2g^{-1})
GPL_{Ref}	141.20
C0-GPL	90.15
C1-GPL	120.30
C2-GPL	180.95
C4-GPL	230.25
C8-GPL	260.67

higher than that of the GPL_{Ref} were obtained after 2 cycles of microfluidization (Table 2). Moreover, it has been observed that the microfluidized GPLs have a more uniform size distribution compared to GPL_{Ref} and C0-GPLs, which have significant size differences.

Figure 3 and Table 3 present the Raman spectra and the I_D/I_G ratios of the GPLs, respectively. I_D/I_G ratios were calculated based on the D- and G-band intensities in Raman spectra. In this study, at least ten Raman analyses were performed on each GPL, and the average values are used in Table 3. As the number of microfluidization cycles increased, the increasing I_D/I_G ratio (Table 3) showed that the microfluidization process led to degradation in the structure of the GPLs [21, 22]. This pointed out that it would be ideal for applying a small number of microfluidization cycles to the C0-GPL to achieve the reinforcement level of GPL_{Ref}.

The average I_{2D}/I_G ratio of the GPL_{Ref} (0.950), as well as the lowest (0.840) and highest (1.000) ratio indicated that it contains both multi-layered and few-layered structures [18]. The I_{2D}/I_G ratios obtained using the Raman spectra of the GPLs were presented in the previous study [19]. According to the average I_{2D}/I_G

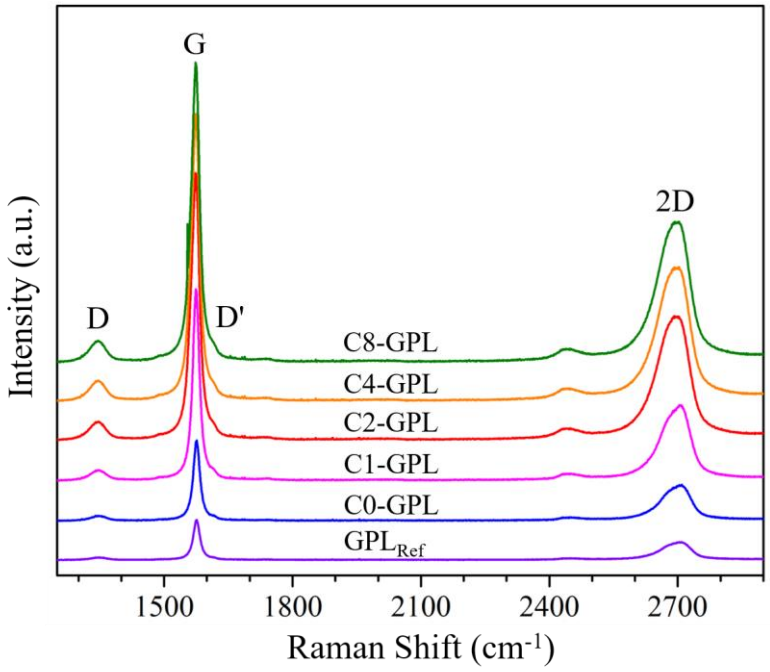

Figure 3. *Raman spectra of the GPL_{Ref}, non-microfluidized C0-GPL and C1-, C2-, C4- and C8-GPLs [18].*

Table 3. *Average I_D/I_G values calculated by using at least ten Raman measurements from GPL_{Ref}, non-microfluidized GPLs and GPLs microfluidized at 1, 2, 4 and 8 cycles. The values in brackets are for the measurements range [18].*

GPLs	**Average I_D/I_G**
GPL_{Ref}	0.820 (0.590-0.970)
C0-GPL	0.840 (0.730-0.950)
C1-GPL	0.850 (0.800-0.955)
C2-GPL	0.870 (0.820-0.960)
C4-GPL	0.920 (0.880-0.980)
C8-GPL	0.960 (0.890-0.987)

value (0.870) of the C0-GPL and its lower (0.770) and upper (0.980) ratio limits, it consists of GPLs that are thicker than the GPL_{Ref} [21,22]. As the number of microfluidization cycles applied to C0-GPL increased, the increase in the average I_{2D}/I_G ratio showed that the GPL agglomerates dispersed, and a part of them became thinner (few-layered) structures. However, it was determined that the average ratio value of C1-GPL was still lower than the GPL_{Ref} [18,19]. This showed that applying 1 cycle of microfluidization to C0-GPL was insufficient to achieve the GPL_{Ref}'s thickness distribution. When 2 cycles of microfluidization were applied to C0-GPL, the I_{2D}/I_G ratio value (0.960) exceeded that of GPL_{Ref}. While this increase in I_{2D}/I_G ratio value was rapid up to 4 cycles of microfluidization, there was no significant difference between the ratios of 4 (0.990) and 8 (0.992) cycles of microfluidized GPLs. When the I_{2D}/I_G ratios [19] and morphological images (Fig. 2) of the GPLs are evaluated together, it is concluded that the microfluidization applied in more than 4 cycles breaks down the GPLs in x- and y- directions rather than thinning or dispersing.

Since the through-plane and in-plane directions microstructures presented in the previous study [10] explained the distribution and orientation of SiAlON grains and GPLs, only in-plane direction BSE-SEM images of the samples were taken in this study. BSE-SEM images of the SiAlON matrix (a) and SiAlON matrix composites containing 1.5 wt % GPL_{Ref} (b), C0-GPL (c) and GPLs microfluidized at different cycles (d-g) are given in Figure 4. The predominantly distribution of the α-SiAlON and basal planes of β-SiAlON grains in the in-plane direction microstructures indicated that some of the elongated surfaces of the β-SiAlON grains were oriented perpendicular to the SPS pressing axis (Fig. 4 a). In addition, it has been observed that α-, β-SiAlONs and liquid phase are homogeneously dispersed without porosity in the microstructure of SiAlON matrix. Microstructures of composites containing GPL_{Ref} and C0-GPL also showed that C0-GPL was thicker than GPL_{Ref}, which supported the Raman analysis. As a result, C0-GPLs (Fig. 4 c) have formed GPL clusters and GPL-poor regions in the matrix microstructure, resulting in less homogeneous distribution than GPL_{Ref} (Fig. 4 b).

While the platelet size reduction of C0-GPL with the microfluidization process was slightly evident up to 2 cycles, it became very pronounced after 4 cycles. It has been observed that the distribution of C1-GPL in the matrix microstructure was more homogeneous than that of C0-GPL, and became almost similar to the distribution of $GPLs_{Ref}$. However, microstructures also showed that C1-GPLs still contained thicker GPLs than GPL_{Ref}, as noted in Raman analyses [19]. The size distributions of C2-GPLs were more uniform than GPL_{Ref}, C0-GPL, and C1-GPL. Additionally, C2-GPL's distribution in the matrix microstructure was also more homogeneous than those of GPL_{Ref}, C0-GPL, and C1-GPL. The reduction in the size of the C4-GPL and C8-GPLs was quite distinct when compared to the C2-GPL. However, there was no significant difference between the distributions of the C2-GPL, C4-GPL and C8-GPL in the matrix microstructure. In addition to all these, there was no porosity in the microstructures of all GPL-SiAlON composites as in

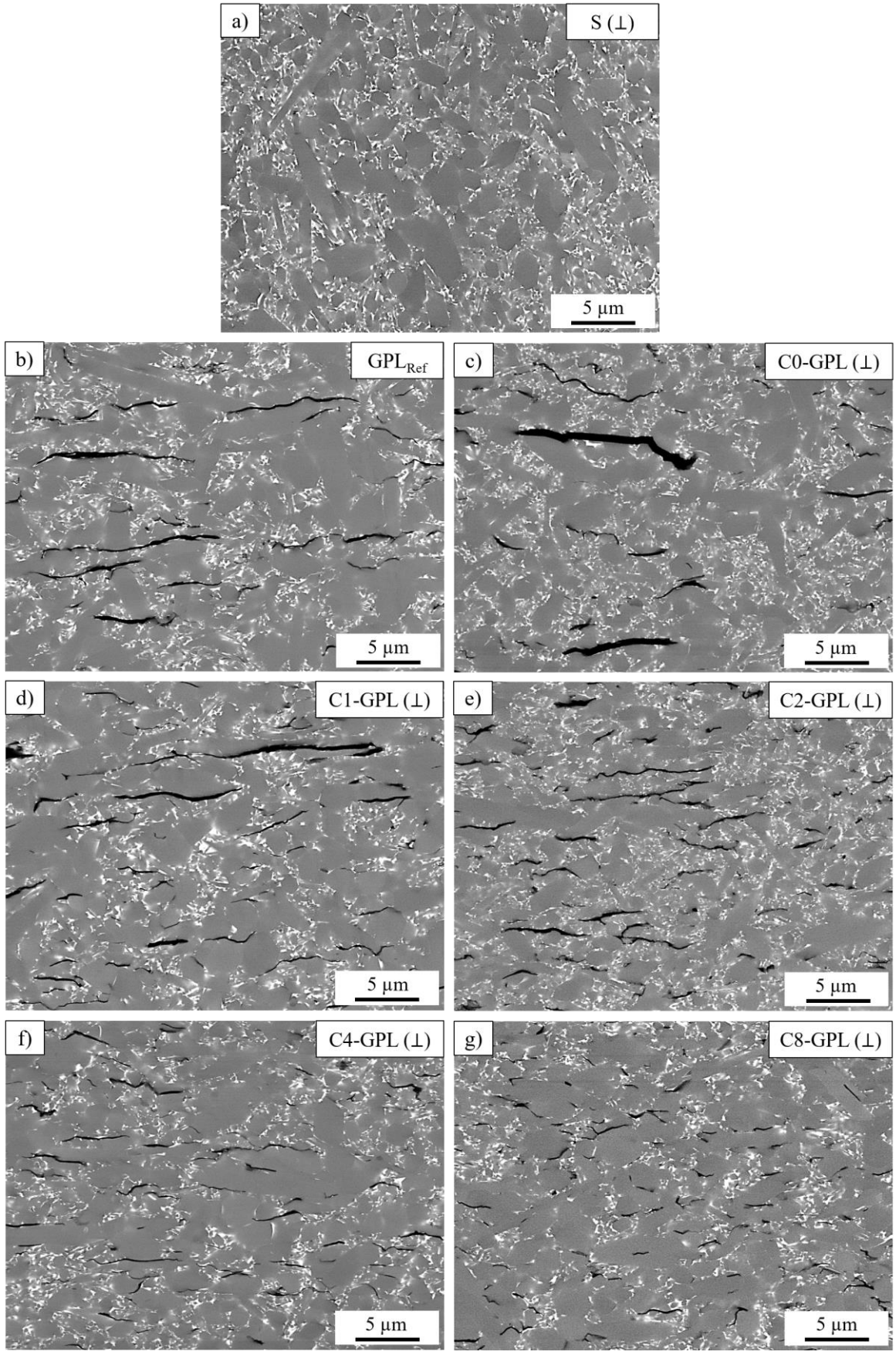

Figure 4. *In-plane direction (⊥) BSE-SEM images of the (a) SiAlON matrix and SiAlON matrix composites containing 1.5 wt % (b) GPL_{Ref}, (c) C0-, (d) C1-, (e) C2-, (f) C4- and (g) C8-GPLs [10,18].*

SiAlON matrix. BSE-SEM images taken in the in-plane direction indicated that the most of GPLs oriented in the SiAlON matrix microstructure with their basal planes perpendicular to the SPS pressing axis.

Table 4 shows the bulk and relative density values of the SiAlON matrix and GPLs-SiAlON composites. The relative density of the SiAlON matrix was accepted as 100 % as no porosity was found in its microstructure (Fig. 4 a). However, the bulk density of the SiAlON matrix decreased slightly by ~ 1 % with the addition of 1.5 wt % GPLs. The porosities caused by elastic modulus/thermal expansion coefficient mismatches between GPLs and SiAlON and the lower density of GPLs compared to the SiAlON matrix may be the reason for this decline. However, the relative densities higher than 99 % and microstructures of GPL-SiAlON composites indicated that they are highly dense materials.

Table 4. *Bulk and relative density values of the SiAlON matrix and SiAlON matrix composites containing 1.5 wt % GPL_{Ref}, C0-, C1-, C2-, C4- and C8-GPLs [18].*

Materials	**Bulk Density (gcm^{-3})**	**Relative Density (%)**
SiAlON	3.240	100.00
GPL_{Ref}/S	3.200	99.50
C0-GPL/S	3.210	99.50
C1-GPL/S	3.215	99.70
C2-GPL/S	3.218	99.80
C4-GPL/S	3.211	99.56
C8-GPL/S	3.195	99.10

3.2. MECHANICAL PROPERTIES

Figure 5 shows the (a) hardness and (b) fracture toughness values of SiAlON matrix and SiAlON matrix composites containing GPL_{Ref}, C0-, C1-, C2-, C4- and C8-GPL in the through-plane and in-plane directions. The hardness value of SiAlON matrix in the through-plane direction was ~ 8 % higher than the in-plane direction hardness value. This result is consistent with the results obtained by Santos et al. [23], who measured the hardness values of hot pressed Si_3N_4 ceramics. The authors [23], who achieved weak orientation in their studies, found the hardness value of 16.30 GPa on the surface (c-axis) parallel to the elongated surfaces of the β-Si_3N_4 grains, while it has found 15.90 GPa on the perpendicular surface (a, b axis). On the other hand, the fact that the hardness value in the through-plane direction of GPLs-SiAlON composites was slightly higher than the values in the in-plane direction and this difference was lower than that of the SiAlON matrix indicated almost isotropic hardness behavior.

The hardness of the SiAlON matrix decreased by about 15 % with the addition of 1.5 wt % GPLs. One of the main reasons for this decrease in hardness is that GPLs have a lower hardness value than SiAlON. In addition, the tendency of GPLs to agglomerate and, in this case, the weak interfacial bonds with SiAlON grains are the parameters that negatively affect the hardness values.

The fracture toughness of the SiAlON matrix in the through-plane direction was ~ 5 % higher than in the in-plane direction. This can be attributed to the lying of the elongated surfaces of β-SiAlON grains in this plane perpendicular to the through-plane direction. On the other hand, with the addition of GPL_{Ref}, the fracture toughness values of the SiAlON matrix in the in-plane and through-plane directions improved by about 24 and 6 %, respectively. Further, the addition of C0-GPL improved the fracture toughness values of the SiAlON matrix by ~20 and 4 % in the in-plane and through-plane directions, respectively. It was observed that the in-plane and through-plane directions toughness values of SiAlON matrix increased by ~

22, 28, 14 and 6 %, and by ~ 6, 14, 7 and 0.7 % with the addition of C1-, C2-, C4- and C8-GPLs, respectively. Among the microfluidized GPLs, C2-GPL increased the fracture toughness of the SiAlON matrix the most in both directions. In the composites containing microfluidized GPLs, the fracture toughness increased up to 2 cycles and decreased as cycle numbers increased (Fig. 5 b). Since C2-GPL is

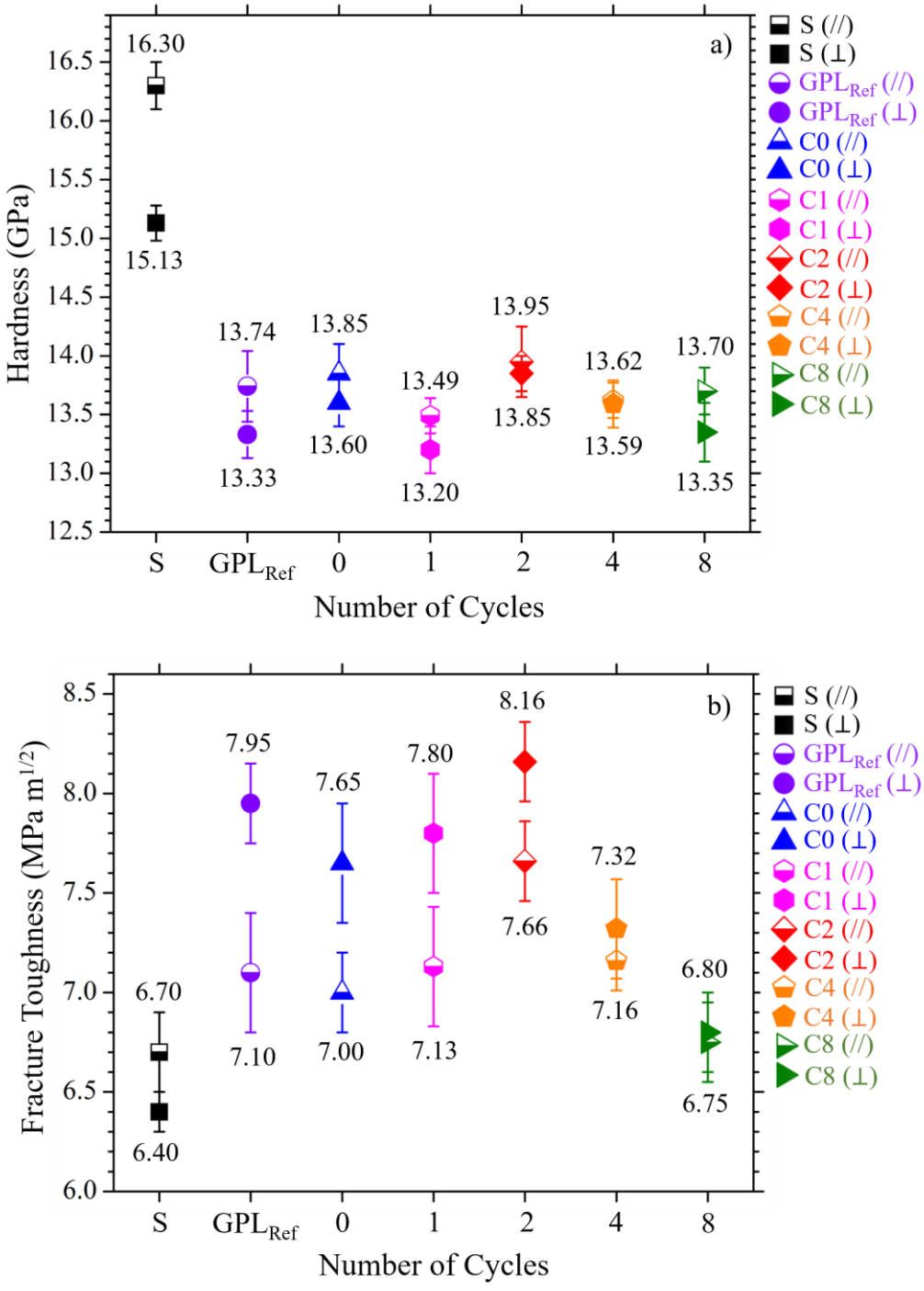

Figure 5. *(a) Hardness and (b) fracture toughness values of the SiAlON matrix and SiAlON matrix composites containing 1.5 wt % GPL$_{Ref}$, C0-, C1-, C2-, C4-, C8-GPLs in the through-plane (//) and in-plane (⊥) directions [18].*

thinner than C0-GPL and C1-GPL, their more homogeneous distribution in the matrix microstructure ensures that the fracture toughness of the composite containing C2-GPL is higher than the others. When

GPLs are homogeneously dispersed in the matrix, the crack encounters more GPLs as it progresses. The realization of more toughening mechanisms such as crack deflection and bridging (Fig. 6) positively affects fracture toughness [14]. On the other hand, although the dispersion levels of C2-GPL, C4-GPL, and C8-GPL were almost similar in the SiAlON matrix, C2-GPL had the highest fracture toughness performance, indicating the positive effect of large platelet size. Larger GPLs delay crack propagation more than smaller ones [10, 24].

It was also observed that the fracture toughness of the composite containing C2-GPL was higher than those containing GPL_{Ref} in both directions. The most obvious reason for this was that C2-GPLs were more homogeneously dispersed in the matrix microstructure, due to the fact that they contained thinner GPLs than GPL_{Ref}. Although the size of C2-GPL is ~ 25 % smaller than GPL_{Ref}, this difference in platelet size did not adversely affect the fracture toughness performance it provides to SiAlON. Another reason why the fracture toughness of SiAlON containing C2-GPL was higher than that containing GPL_{Ref} was that it had a more uniform platelet size distribution.

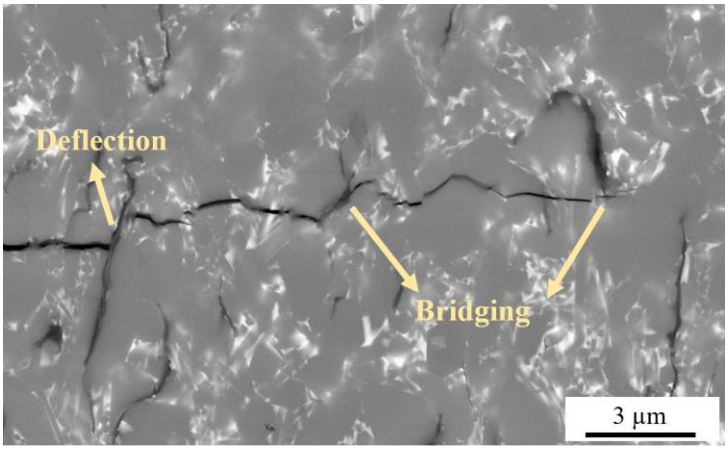

Figure 6. *Toughening mechanisms took place along a portion of a representative crack in the SiAlON matrix composite containing C2-GPL in the in-plane (⊥) direction.*

Following the determination that SiAlON containing 1.5 wt % C2-GPL has the highest fracture toughness, SiAlON matrix composites containing 0.5 and 1 wt % C2-GPL were produced to investigate whether the fracture toughness could be further increased without affecting the hardness of SiAlON. Figure 7 shows the fracture toughness behavior of SiAlON composites containing 0.5, 1 and 1.5 wt % C2-GPL. The fracture toughness values of SiAlON in the in-plane and through-plane directions increased by ~13, 36 % and ~ 5 , 25 %, with the addition of 0.5 and 1 wt % C2-GPLs, respectively. C2-GPL/SiAlON composites had the highest fracture toughness value among themselves at 1 wt % C2-GPL content. In the previous study [10], when 1 wt % GPL_{Ref} was added to SiAlON, the highest toughness value was reached, and a toughness increase of ~33 and 21 % in the in-plane and through-plane directions, respectively. The addition of C2-GPL increased the toughness value of SiAlON more than GPL_{Ref} in both directions.

The fracture toughness values of all GPL-SiAlON composites were higher in the in-plane direction than in the through-plane direction due to the orientation of the GPLs in the matrix microstructuresf (Fig. 5 b). However, this difference has decreased as the platelet sizes of the GPLs have decreased. This can be explained by the decreasing tendency of the GPLs to orient in the matrix microstructure as the platelet sizes get smaller [10].

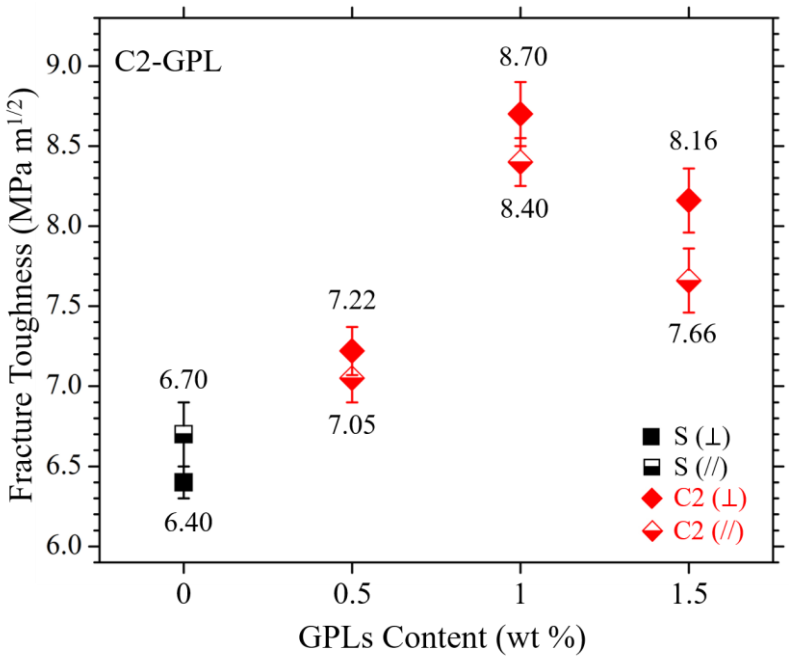

Figure 7. *Through-plane and in-plane directions fracture toughness values of SiAlON matrix composites containing 0.5, 1 and 1.5 wt % C2-GPL [18].*

4. CONCLUSION

In this study, it was investigated whether the mechanical reinforcement performance of GPL_{Ref}, which is commercially expensive as a result of its good exfoliation and has been found to improve the fracture toughness of SiAlON significantly, can be achieved economically. For this, it was aimed to thin the C0-GPL, which has the same platelet size as GPL_{Ref} but is thicker and cheaper, to provide homogeneous dispersion at the same level as GPL_{Ref} in the matrix microstructure. A new approach, the microfluidization technique, was used for the thinning/dispersion of C0-GPL. Among the SiAlON matrix composites containing 1 (C1-GPL), 2 (C2-GPL), 4 (C4-GPL) and 8 (C8-GPL) cycles of microfluidized GPLs, the fracture toughness values of the SiAlON containing C2-GPL were found to be higher than those containing GPL_{Ref}. This was because, by applying 2 cycles of microfluidization to C0-GPL, GPLs thinner than GPL_{Ref} could be obtained, resulting in a more homogeneous distribution in the matrix microstructure. Another reason for this was partially preserving the platelet size of the C0-GPL with 2 cycles of microfluidization.

ACKNOWLEDGEMENTS

The Eskisehir Technical University Scientific Research Projects under the project numbers of 1606F570 and 19ADP019 supported this work. Authors would like to thank to MDA Advanced Ceramics Ltd. for providing all the raw materials and to Prof. Dr. A. Tuğrul Seyhan for providing the microfluidization device.

REFERENCES

[1] Singh, V., Joung, D., Zhai, L., Das, S., Khondaker, S.I., Seal, S. (2011). Graphene based materials: past, present and future. Prog. in Mater. Sci., 56, 1178–1271. https://doi.org/10.1016/j.pmatsci.2011.03.003

[2] Mas-Balleste, R., Gomez-Navarro, C., Gomez-Herrero, J., Zamora, F. (2011). 2D materials: to graphene and beyond. Nanoscale, 3, 20-30. https://doi.org/110.1039/C0NR00323A

[3] Geim, A.K., Novoselov, K.S. (2007). The rise of graphene. Nat. Mater., 6, 183–191. https://doi.org/10.1142/9789814287005_0002

[4] Yaping, Y., Bin, L., Changrui, Z., Siqing, W., Kun, L., Bei, Y. (2015). Fabrication and properties of graphene reinforced silicon nitride composite materials. Mat. Sci. & Eng. A, 644, 90-95. https://doi.org/10.1016/j.msea.2015.07.062

[5] Zeng, Z., Liu, Y., Chen, W., Li, X., Zheng, Q., Li, K., Guo, R. (2018). Fabrication and properties of in situ reduced graphene oxide-toughened zirconia composite ceramics. J. of Amer. Ceram. Soc., 101, 3498. https://doi.org/10.1111/jace.15483

[6] Liu, J., Yan, H., Jiang, K. (2013). Mechanical properties of graphene platelet-reinforced alumina ceramic composites. Ceram. Inter., 39 (6), 6215-6221. https://doi.org/10.1016/j.ceramint.2013.01.041

[7] El-Amir, A.A.M., El-Maddah, A.A., Ewais, E.M.M., El-Sheikh, S.M., Bayoumi, I.M.I., Ahmed, Y.M.Z. (2021). Sialon from synthesis to applications: an overview. J. of Asian Ceram. Soc., 9 (4), 1390-1418. https://doi.org/10.1080/21870764.2021.1987613

[8] Hoffmann, M.J. (2011). Si_3N_4-Ceramics, Structure and Properties of, Encyclopedia of Materials. Sci. and Tech. https://doi.org/10.1016/B0-08-043152-6/01513-8.

[9] Ekström, T., Nygren, M. (1992). SiAlON ceramics. J. of Amer. Ceram. Soc., 75, 259–276. https://doi.org/10.1111/j.1151-2916.1992.tb08175.x

[10] Baskut, S, Sert, A., Çelik, O.N., Turan, S. (2021). Anisotropic mechanical and tribological properties of SiAlON matrix composites containing different types of GNPs. J. of the Europ. Ceram. Soc., 41, 1878–1890. https://doi.org/10.1016/j.jeurceramsoc.2020.10.071

[11] Taylor, A.C. (2012). Processing of polymer nanocomposites. Manufac. Tech. for Poly. Mat. Comp. (PMCs), 95-119. https://doi.org/10.1533/9780857096258.1.95

[12] Porwal, H., Tatarko, P., Grasso, S., Khaliq, J., Dlouhý, I., Reece, M.J. (2013). Graphene reinforced alumina nano-composites. Carbon, 64, 359-369. https://doi.org/10.1016/j.carbon.2013.07.086

[13] Yun, C., Fenga, Y., Qiu, T., Yang, J., Li, X., Yu, L. (2015). Mechanical, electrical, and thermal properties of graphene nanosheet/aluminum nitride composites. Ceram. Inter., 41(7), 8643-8649. https://doi.org/10.1016/j.ceramint.2015.03.075

[14] Tapasztó, O., Puchy, V., Horváth, Z.E., Fogarassy, Z., Bódis, E., Károly, Z., Balázsi, K., Dusza, J., Tapasztó, L. (2019). The effect of graphene nanoplatelet thickness on the fracture toughness of Si_3N_4 composites. Ceram. Inter., 45(6), 6858-6862. https://doi.org/10.1016/j.ceramint.2018.12.180

[15] https://www.beei.com/blog/microfluidization-how-does-it-work

[16] https://www.microfluidics-mpt.com/microfluidics-technology/how-it-works.

[17] Yurdakul, H., Göncü, Y., Durukan, O., Akay, A., Seyhan, A.T., Ay, N., Turan, S. (2012). Nanoscopic characterization of two-dimensional (2D) boron nitride nanosheets (BNNSs) produced by Microfluidization. Ceram. Inter., 38, 2187-2193. https://doi.org/10.1016/j.ceramint.2011.10.064

[18] Başkut, S. (2019). The Effect of Different Graphene Nanoplatelets Addition on Mechanical,Thermal and Electrıcal Properties of SiAlON Ceramics, PhD Thesis, Eskisehir Technical University, Institute of Graduate Programs.

[19] Başkut, S., Turan, S. (2022). The Effects of Applying Microfluidization at Different Cycles on the Properties of Graphene Platelets. 8th International Istanbul Scientific Research Congress, 505-509. ISBN: 978-605-71167-8-9

[20] Rangel, E.R. (2011). Fracture Toughness Determinations by Means of Indentation Fracture, Nanocomposites with Unique Properties and Applications in Medicine and Industry. InTech. ISBN:978-953-307-351-4.

[21] Childres, I., Jaureguib, L.A., Park, W., Cao, H., Chen, Y.P. (2010). Raman spectroscopy of graphene and related materials. 97, 173109.

[22] Wall, M. The raman spectroscopy of graphene and the determination of layer thickness. Thermo Fisher Scientific, Application Note: 52252.

[23] Santos, C., Strecker, K., Baldacim, S.A., da Silva, O.M.M., da Silva, C.R.M. (2004). Influence of additive content on the anisotropy in hot-pressed Si_3N_4 ceramics using grain orientation measurements. Ceram. Inter., 30 (5), 653-659. https://doi.org/10.1016/j.ceramint.2003.07.011

[24] Chatterjee, S., Nafezarefi, F., Tai, N.H., Schlagenhauf, L., Nüesch, F.A., Chu, B.T.T. (2012). Size and synergy effects of nanofiller hybrids including graphene nanoplatelets and carbon nanotubes in mechanical properties of epoxy composites. Carbon, 50, 35380–5386. https://doi.org/10.1016/j.carbon.2012.07.021

[25] Başkut, S., Turan, S. (2020). The effect of different GNPs addition on the electrical conductivities and percolation thresholds of the SiAlON matrix composites. J. of the Europ. Ceram. Soc., 40 (4), 1159-1167. https://doi.org/10.1016/j.jeurceramsoc.2019.11.057